CODEN STJSAO
ZX470/1485

ISSN 0562-1887
UDK 628.85/.87:697.97:532.525:519.63(043)

Experimental Analysis of Thermal Comfort in an Air Conditioned Open Space Office*

Igor WOLF

Tehnički fakultet Sveučilišta u Rijeci
(Faculty of Engineering University of Rijeka),
Vukovarska 58, HR-51000 Rijeka,
Republic of Croatia

igor.wolf@riteh.hr

Keywords
Air distribution
Laser-Doppler-Anemometry
Thermal comfort
Turbulent wall jets

Ključne riječi
Laser-Doppler-anemometriranje
PMV-PPD model
Toplinska ugodnost
Turbulentni površinski mlazovi

Received (primljeno): 2010-07-08
Accepted (prihvaćeno): 2010-10-29

Original scientific paper

Experimental analysis of thermal comfort in an open plan office has been presented in the paper. The office of interest is air conditioned by two parallel ceiling air terminal devices (ATDs). With the aim of mathematical description of the main characteristics of turbulent wall jets produced by the ATDs, a set of experimental measurements was carried out using the laser-Doppler-anemometer (LDA) method. Velocity profiles in the jets, axial velocity decay and other relevant jet characteristics were investigated for three distances between the ATDs and three fan speeds. For all nine cases, in the second phase of the measurements temperature and velocity fields within the occupied zone were determined and thermal comfort evaluated. The measurements were carried out in a full-scale test room at the Faculty of Engineering University of Rijeka.

* Defended Doctoral Thesis (2010)

Pokusna analiza toplinske ugodnosti klimatiziranoga otvorenoga uredskog prostora

Izvornoznanstveni rad

U radu je izvršena pokusna analiza toplinske ugodnosti uredskoga prostora klimatiziranoga istovremenim radom dvaju podstropnih, paralelnih terminalnih uređaja. S ciljem matematičkoga opisa značajki turbulentnih površinskih mlazova proizvedenih radom terminalnih uređaja, metodom laser-Doppler-anemometriranja (LDA) izvršen je čitav niz pokusnih mjerenja. Istraženi su profili brzina u mlazovima, opadanje maksimalne brzine i druge relevantne značajke, za tri različite udaljenosti između terminalnih uređaja i za tri brzine vrtnje ventilatora. Za svih devet analiziranih slučajeva, u drugoj fazi mjerenja utvrđena je raspodjela temperaturnih i polja brzina unutar zone boravka, te je ocijenjena razina toplinske ugodnosti. Sva su mjerenja odrađena na modelu uredskoga prostora stvarne veličine, na Tehničkome fakultetu Sveučilišta u Rijeci.

* Obranjena doktorska disertacija (2010.)

1. Introduction

People spend more than 90 % of their time in enclosed spaces [1]. A large fraction of that time is spent in different kinds of offices. Many conducted researches have emphasized the necessity of providing adequate indoor air quality and thermal comfort to office employees to keep them healthy and promote their productivity [2,3]. Creation of a comfortable indoor environment, except for proper air cooling or heating to achieve the required temperature and humidity, almost completely depends on space air distribution.

Office air conditioning is most commonly based on a mixed air diffusion scheme. A properly designed mixing system produces a relatively uniform air quality and thermal conditions within the occupied zone, maintaining a desired set-point temperature and velocities low enough to avoid the feeling of draught. The conditioned air is distributed by turbulent jets discharged from different types of air terminal devices (ATDs) at velocities much greater than those acceptable for a comfortable stay to promote mixing with the room air. A conditioned air temperature may be above, below, or equal to the air temperature in the occupied zone, depending on the heating/cooling load. The discharged jets mix with the room air by entrainment, which decays the initial jet velocity and equalizes the air temperature.

Physical conditions produced by a mixing system are affected by the throw characteristics of ATDs, their type and placement, room size and geometry, supply air temperature, initial air velocity, room temperature, heat loads in the room, heating or cooling operation, radiant heat from the walls, furniture placement and pollutant sources. All these factors cause the mixing system to

Symbols/Oznake

A_0 - effective area of jet at discharge, m²
- efektivna površina mlaza kod istrujavanja

Ar - Archimedes number
- Arhimedova značajka

f_{cl} - clothing area factor
- faktor površine odjeće

g - gravitational acceleration, m/s²
- ubrzanje Zemljine sile teže

h_0 - effective height of an ATD opening, m
- efektivna visina otvora terminalnoga uređaja

K - maximum (centreline) velocity decay coefficient
- koeficijent opadanja maksimalne brzine

l_0 - effective length of an ATD opening, m
- efektivna duljina otvora terminalnoga uređaja

M - rate of metabolic heat production, W/m²
- metabolički učinak

n - maximum velocity decay exponent
- eksponent opadanja maksimalne brzine

p_{air} - water vapour pressure in ambient air, Pa
- tlak vodene pare u zraku

Re - Reynolds number
- Reynoldsova značajka

T_I - turbulence intensity, %
- intenzitet turbulencija

$\dot{V}_{air}$ - supply air flow rate, m³/h
- protok dovodnoga zraka

W - rate of mechanical work accomplished, W/m²
- izvršeni mehanički rad

w_0 - initial jet velocity, m/s
- početna brzina mlaza

w_m - maximum jet velocity at distance x, m/s
- maksimalna brzina u mlazu na udaljenosti x

w_{sd} - standard deviation of the velocity measured, m/s
- standardna devijacija brzine

w_x - velocity at distance z from the centreline, m/s
- brzina na udaljenosti z od osi mlaza

x - distance from the ATD to a point of centreline velocity measurement, m
- udaljenost na osi mlaza od terminalnoga uređaja do mjesta mjerenja brzine

$z_{0.5}$ - distance from the ceiling where $w_x = 0.5\ w_m$, m/s
- udaljenost od stropa na kojoj je $w_x = 0.5\ w_m$

α_c - convective heat transfer coefficient, W/m²K
- koeficijent konvekcijskoga prijelaza topline

β - thermal expansion coefficient, 1/K
- koeficijent temperaturnoga rastezanja

ϑ_{cl} - temperature of the outer clothing surface, °C
- temperatura vanjske površine odjeće

ϑ_o - operative temperature
- osjetna temperatura

$\overline{\vartheta}_r$ - mean radiant temperature, °C
- srednja temperatura zračenja ploha prostora

ϑ_0 - initial air temperature, °C
- temperatura primarnoga zraka

$\Delta\vartheta$ - temperature difference between primary and room air, °C
- temperaturna razlika primarnog i zraka u prostoru

v - kinematic viscosity, m²/s
- kinematički viskozitet

Φ - spread angle of a jet, °
- kut širenja mlaza

produce different airflow patterns. The resulting airflow patterns influence temperature and velocity distributions and contaminant removal within the occupied zone, and, therefore, have a significant impact on the occupants' satisfaction with the environment.

Today's office planning policy is often directed to open plan design. From the HVAC system designing point of view, open space offices are challenging because they encompass large(r) number of workstations, they are shared by diverse occupants having different needs and expectations regarding thermal comfort and indoor air quality, and heat and pollution sources are multiple and distributed in space. To create a uniform thermal environment, several ATDs are needed. During simultaneous operation, the jets discharged can interact and create undesirable and, in the HVAC systems design phase, hardly predictable air velocity and temperature distributions within the space.

Mechanical ventilation and air conditioning systems consume more than 55 % of overall energy consumption in commercial buildings [4-5]. To conserve energy, performances of these systems must be optimized. Optimization of a building HVAC system must minimize energy consumption but preserve high indoor thermal and air quality conditions. This goal can only be achieved using reliable numerical models. Such tools help designers to predict a level of attainable thermal comfort in single rooms, to predict overall building's energy consumption and to select optimal HVAC system and its components. To simplify the usage of numerical models to HVAC designers, macroscopic (TRNSYS, DOE, ESP, etc.) and zonal models have been developed [6-7]. The aim of zonal models is to provide more details of room airflow patterns for whole building simulation studies in a way that is computationally and professionally less demanding than CFD models. They critically rely on empirical constants and correlations, which must be found on the basis of reliable experimental investigations.

The aim of the present research was to investigate air movement patterns and their impact on thermal comfort

for the case of an open space office air conditioned by two parallel, ceiling ATDs. The research was divided into two phases. In the first phase, emphasis was placed on determining the main characteristics of three-dimensional wall jets discharged from the selected type of ATDs. In the second phase, resulting air velocity and temperature distributions within the occupied zone were investigated and the achieved thermal comfort level evaluated. Experimental measurements were carried out in the Laboratory of Heating, Ventilating and Air Conditioning at the Faculty of Engineering University of Rijeka, in a full-scale test room, for three distances between the ATDs and three fan speeds (i.e. initial air velocities).

2. Air jet theory and characteristics

To design proper air diffusion, it is essential to fully understand air jet behaviour downstream of an ATD. Air diffusion in the further field from the ATD greatly depends on its design [8], on type, direction and characteristics of spread of the jet produced, on jet's flow rate and its temperature differential to the room air. The behaviour of a jet is also influenced by its interaction with walls, adjacent jets, plumes and various barriers. The aim of the air jet theory is to try to predict jets behaviour under certain operating conditions, in order to be able to assess the resulting flow patterns and predict velocities and temperatures within the occupied zone. The occupied zone represents that volume of a room in which it is necessary to provide comfortable physical conditions. It is the space 1 m away from the external wall(s) and 0.5 m away from the inner walls. Its height equals the height of a standard man (1.80 m) [9].

The flow of a jet differs from other kinds of fluid flow because a jet is surrounded on one or more sides by a free boundary of the same fluid. The interaction between the flow within the jet and the boundary, the process known as entrainment, has a major influence on the development of the flow in the jet. As a free jet (i.e. a jet not obstructed by walls, ceiling or other obstructions) leaves the ATD, a free shear layer develops around its boundary as a result of the velocity discontinuity at the boundary. The thickness of the free shear layer increases with axial distance until the central region, the potential core region, is completely consumed. Downstream from the core the flow becomes more turbulent and the centreline velocity decreases. Depending on how its centreline velocity decays with distance from the ATD, the flow of a free jet can be divided into four zones (Figure 1), briefly described in the following section [10].

Zone 1: Potential core region

In this region, immediately downstream from the ATD, mixing of the jet with the surrounding air is not complete. The centreline (maximum) velocity w_m is constant and equal to the initial velocity w_0.

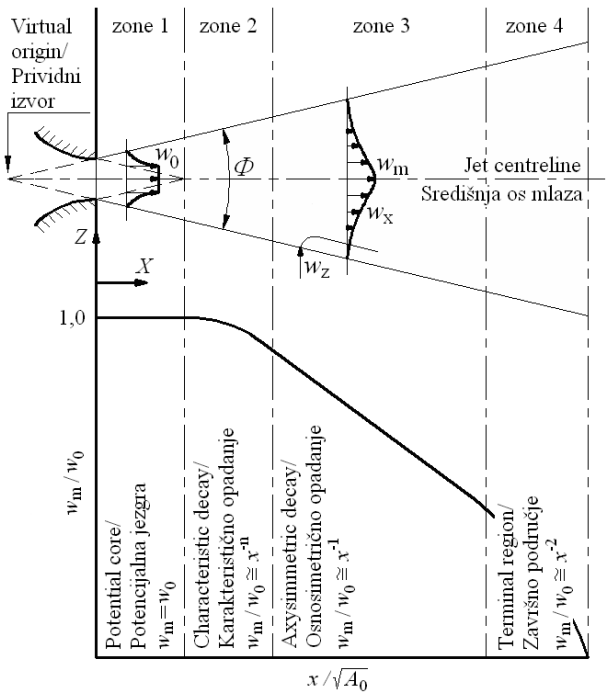

Figure 1. Decay regions of a free jet
Slika 1. Zone raspada slobodna mlaza

Zone 2: Characteristic decay (transitional) region

After the potential core has been consumed by the free shear layer, the centreline velocity begins to decay so that

$$w_m / w_0 = K_2 \, x^{-n}, \tag{2}$$

where x is the distance from the ATD and n is an index which has a value between 0.33 and 1.0. The value of n depends on the shape of the ATD. It is usually associated with large aspect ratio ATDs ($l_0/h_0 > 40$).

Zone 3: Axisymmetric decay (main) region

For three-dimensional free jets (small aspect ratio ATDs, $1 < l_0/h_0 < 40$) this is the predominant region. The flow here is considered to be fully developed and the spread angle of the jet is a constant whose value depends on the geometry of the ATD. A cross section of the jet is always circular, regardless of the shape of the ATD. This region is dominated by a highly turbulent flow generated by viscous shear at the edge of the shear layer. In the majority of cases, the air jet enters the occupied zone in this region. The centreline velocity decays inversely with the distance from the ATD,

$$w_m / w_0 = K_3 \, x^{-1}. \tag{3}$$

Zone 4: Terminal region

In this region of rapid and complete decay, the jet becomes indistinguishable from the surrounding air. The characteristics of this zone are not well known. The centreline velocity decays with the square of the distance,

$$w_m / w_0 = K_4 \, x^{-2}. \quad (4)$$

The length of each of the zones depends on the geometry of the ATD and, to a lesser extent, on the turbulence characteristics at the ATD. Large aspect ratio ATDs produce plane or 2D jets in which zones 1 and 2 are dominant. On the other hand, smaller aspect ratio ATDs produce axisymmetric or 3D jets in which zones 1 and 3 are dominant [10].

Air motion in the occupied zone is primary affected by the jets discharged from ATDs. The interaction between the supply airstream and the room air or a nearby wall produces turbulences in the flow. These turbulences are further transported within the room. Despite the fact that turbulences are weakened by shear stresses caused by the interaction with slower air layers, they are still intense enough to cause discomfort. Mixing air distribution systems are, therefore, usually based on ceiling-mounted ATDs. With an appropriate design solution, air discharged attaches to the ceiling due to the Coanda effect. A wall jet is produced that remains attached to the ceiling for a distance dependent on the initial jet velocity and temperature differential to the room air. Higher air velocities are kept near the ceiling and good mixing of primary and secondary air away from the occupied zone prevents the filling of draught.

To predict air velocity and temperature distributions within the occupied zone, air jet characteristics must be mathematically described and quantified. The most important characteristics of a jet are its throw, spread, velocity profiles at different distances from a supply ATD, centreline velocity decay and drop. The throw is defined as the horizontal or vertical axial distance an airstream travels after leaving the ATD before the centreline velocity is reduced to a specified terminal velocity (for example, 0.25 m/s). The spread is normal divergence of a jet as it leaves the ATD and entrains the surrounding air. The drop is the vertical distance that the lower edge of a horizontally projected airstream drops between the ATD and the end of its throw. The temperature difference between the supply and the room air generates buoyancy forces in the jet, which affect its trajectory, the location of its separation from the ceiling and its throw. Jet's drop depends also on the initial velocity and on the size and shape of the ATD. The significance of such effects depends on the ratio of thermal buoyancy and inertial forces, characterized by Archimedes number.

Experimentally, air jet characteristics are determined by measuring velocities at several points located at various distances from an ATD.

3. Experimental measurements

The measurements were carried out in the Laboratory of Heating, Ventilating and Air Conditioning at the Faculty of Engineering University of Rijeka. A test room (10 m long, 5 m wide and 3 m high) was prepared so that it represented an open plan office in a multi-storey building. The experiments were designed to simulate typical summer office conditions only: the room air temperature was set to 25 °C, while the outdoor air temperature was assumed to be 32 °C. The ground plan of the test room is shown in Figure 2.

The test room was prepared assuming that the office it represented had one external wall with three windows of the same size (1.4 m high and 1.0 m wide). A climate chamber was built next to the test room's imaginary external wall (north wall in Figure 2), in which the

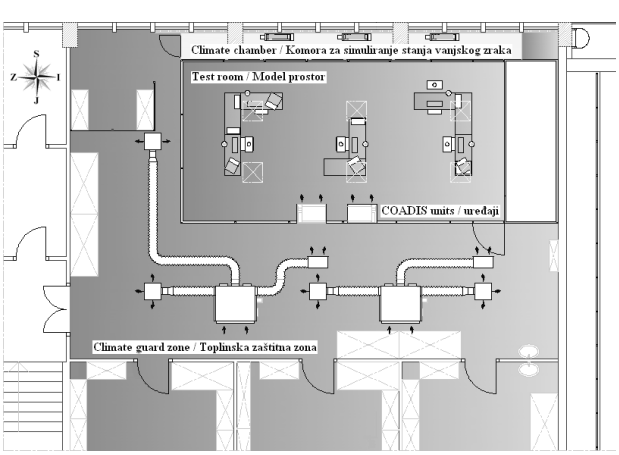

Figure 2. The ground plan of the test room

Slika 2. Tlocrt model-prostora

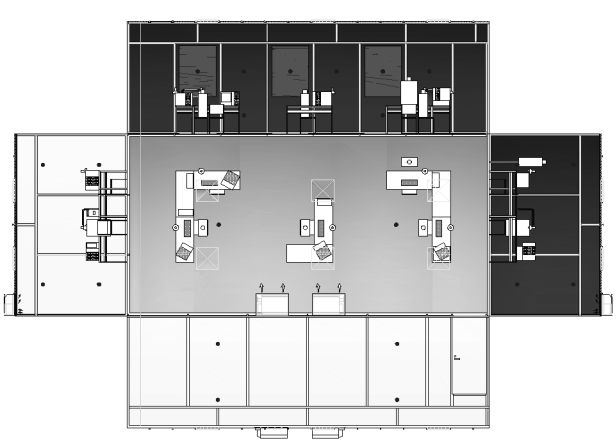

Figure 3. Positions of the thermocouples in the test room (•)

Slika 3. Raspored termoparova u model-prostoru

outdoor air temperature was simulated. The test room was enclosed by all the other sides with a space called climate guard zone that was controlled at a constant air temperature level of 25 °C. That space represented surrounding equally air conditioned rooms.

Tables and chairs were placed in the test room and workstations formed. Real internal heat loads were simulated with four mannequins, four personal computers and lights. The mannequins (just torsos) were wrapped in electric heating cables (heating capacity 100 W) and dressed with a T-shirt and a long sleeve shirt. Three of them were put on chairs and one was left in the standing position. The PCs were put on the tables, together with CRT monitors. Every PC had a power supply unit of 200 W. Total electric power of six fluorescent ceiling lights installed in the room was 432 W. Five table lamps with 150 W bulbs were also used.

The external and internal heat loads were balanced by two ceiling-mounted terminal devices. In the research, COADIS terminal units, manufactured by CIAT, were tested. The COADIS is a hydronic cooling and heating system made for integration in a standard 600 x 600 mm suspended ceiling grid. The COADIS unit should be installed at one end of the ceiling, normally in front of the wall opposing to the windows. The COADIS unit's supply opening is designed as a multi-nozzle grille. The model 235/22 (895 mm long and 595 mm wide) is equipped with 60 high-induction circular nozzles arranged in four rows. The nozzles can be arbitrarily adjusted to optimize the spread pattern of the jet. The nozzles discharge the air horizontally near the ceiling and the Coanda effect is induced. The room air is extracted through a grille integrated in the unit's front panel just behind the nozzles. Three factory-wired fan speeds are available for adjusting the cooling/heating capacity of the unit. In this research, the COADIS units were installed in parallel, just in front of the south wall of the test room (Figure 2). All the nozzles were directed uniformly towards the opposite, external wall.

The water flow rate through the COADIS units was set to balance their cooling capacity and the heat loads in the test room at the middle fan speed and the water temperature regime 7 / 12 °C. Stable temperature conditions in the test room were obtained at the water flow rate 0.23 m^3/h per unit. The water flow rate was manually controlled and measured by two magnetic-inductive flowmeters Sitrans F M MAGFLO MAG 1100F, manufactured by Siemens. The water temperatures were measured and controlled by Honeywell's building management system (BMS) based on a microprocessor controller Excel 500. Air temperatures in the test room and in the adjoining spaces were also measured and controlled by the Honeywell's BMS system. The air temperatures were measured using T7560A and T7460A sensors (NTC thermistors). Their accuracy in the range between 15.5 and 29.5 °C was ± 0.3 °C. Relative humidity of the air in the test room was not controlled but it was measured and recorded by the BMS system. The accuracy of the humidity sensor used (Honeywell H7012A) was ± 2 % in the range of 30-60 %. Relative humidity in the test room was always around 50 %. Inner wall temperatures were measured by 24 K-type thermocouples (Figure 3), which were calibrated in the Laboratory with the accuracy ± 0.3 °C. The thermocouples were connected to a SCXI-type data acquisition system manufactured by National Instruments. The system was guided by an application developed in LabView 6.0.

The measurements were divided into two phases. In the first phase, the velocity profiles in the jets were measured at different horizontal and vertical cross sections of the flow. In the second phase, air velocity and temperature distributions within the occupied zone were determined. Nine tests were carried out in both phases. Three different distances between the COADIS units were tested (645, 945 mm and 1 545 mm) and for each distance three factory-wired fan speeds were used (i.e. initial jet velocities). The distance was changed in such a way that the left unit was kept at its original position, while the second unit was moved to the necessary position.

The two most commonly used velocity measurement techniques in industry and in the scientific community are laser-Doppler-anemometry (LDA) and hot-wire anemometry. Both techniques were used in the research.

3.1. Measurements of velocity profiles

Velocity profiles in the jets were measured using Dantec Dynamics' FlowLite 2D LDA system. The basic components of a LDA system are shown in Figure 4. A thorough description of LDA can be found in [11].

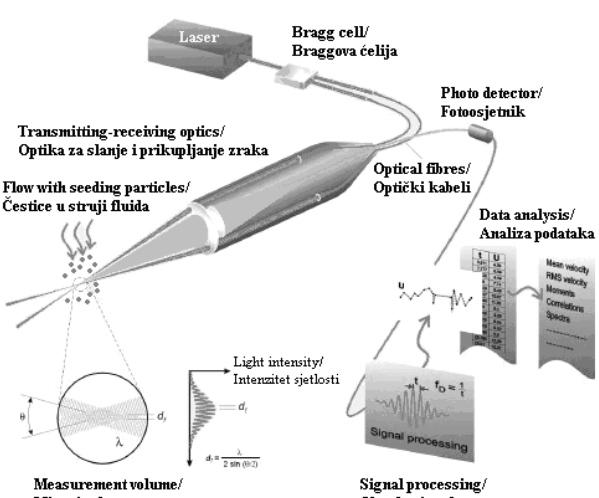

Figure 4. Basic components of a LDA system

Slika 4. Osnovni dijelovi mjernog sustava LDA

The FlowLite 2D LDA system simultaneously measures two velocity components. Two lasers are integrated in the optical system and linked to a LDA probe: a 25 mW Nd:YAG laser generates a beam with a wavelength of 532 nm and a 10 mW He-Ne laser generates a beam with a wavelength of 632.8 nm. The system uses 40 MHz Bragg cells for laser beams splitting and frequency shifting. The optical probe used had a diameter of 60 mm. The front lens focal length was 160 mm. The probe was mounted on a 2D traversing system with the maximum travelling distance of 2 m along both the axes and the positioning accuracy of ± 0.1 mm. The probe was mounted at an angle of 18° to the horizontal plane in order to be able to measure velocities in the region just under the ceiling. Since the test room was wider than the probe travelling distance, the traversing system had to be manually moved to scan the entire test sections. Seeding particles were produced by evaporating the Acetrain's INSTA-MIST Pro Smoke Super ZR Mix solution using an electric heater. The outlet nozzle of the heater was connected to the return grille of one of the COADIS units with a flexible tube. The signals from the photo detectors were processed by a two-channel Burst Spectrum Analyzer (BSA) F60 processor 62N40. The complete LDA system including optics, the BSA processor and the traversing system was controlled from a PC using the BSA Flow Software (version 2.11).

LDA is considered an absolute flow measurement method. It has a very high accuracy, measuring velocity ranging from zero to supersonic order. As the optics of the apparatus was calibrated by the manufacturer, errors associated with them were considered negligible.

The velocities in the jets were measured in three parallel planes shown in Figure 5. In each plane, the velocity profiles were analysed in 11 cross sections starting from the ceiling and ending at the height where the velocity was lower than 0.15 m/s (Figure 6). The measurements in horizontal plane in each cross section were carried out at the height (i.e. distance from the ceiling) at which a maximum velocity in the cross section occurred. Since velocity profiles in the jets discharged from left and right unit were not completely identical at the same fan speed, in each cross section a height was chosen at which the velocities were maximal in both profiles.

3.2. Velocity and temperature measurements in the occupied zone

According to EN ISO 7730, evaluation of thermal comfort in the occupied zone demands the following [12]: calculation of the PMV and PPD indices and operative temperature, determination of radiant temperature asymmetry and vertical air temperature difference, and evaluation of the risk of draught (i.e. calculation of the PD index). Environmental parameters (air velocity, temperature and relative humidity, mean radiant temperature) must be measured at four heights: near the ankles (0.1 m above the floor), at the body centre (0.6 m for a sitting person, 1.1 m for a standing person), and near the head of the occupant (1.1 m for a sitting person, 1.7 m for a standing person).

Air velocity and temperature measurements in the occupied zone were carried out using Dantec Dynamics' omnidirectional transducers 54T21. The transducers measure instantaneous air velocity and temperature in a point and provide two nonlinear analogue voltage signals: one for velocity and one for temperature. The velocity sensor is a miniature constant temperature anemometer

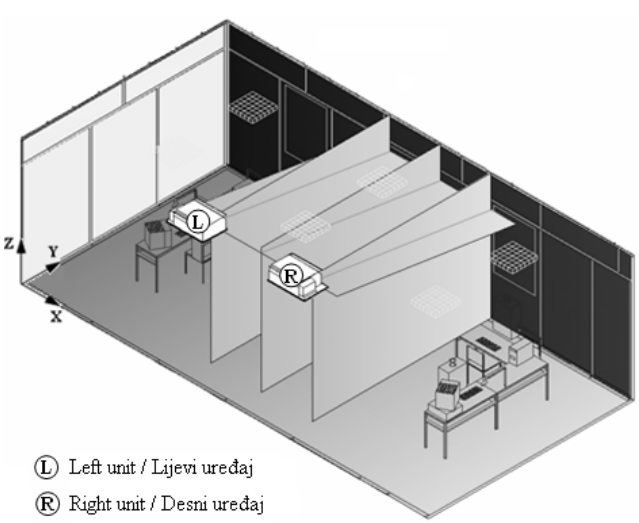

Figure 5. Measuring planes
Slika 5. Mjerne ravnine

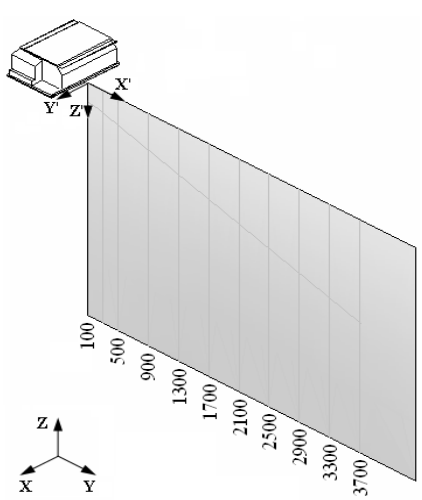

Figure 6. Measuring cross sections
Slika 6. Mjerni presjeci

and the temperature sensor is a microthermistor enclosed in a glass capsule. The transducers were calibrated by the manufacturer with an accuracy of ± 0.02 m/s for velocity measurements and ± 0.2 °C for temperature measurements.

The measurements were carried out at 36 uniformly selected locations in the occupied zone (Figure 7). Since at each location air velocity and temperature were measured at four heights, there were 144 measurement points altogether. Two omnidirectional transducers were available. They were fixed to copper rod mounted on a stand and manually moved within the space. The measurements were simultaneously performed at two heights: at 100 and 600 mm, and at 1 000 and 1 700 mm. When the measurements at all 36 locations for the first two heights were finished, the procedure was repeated for the remaining heights. The measurement in a single point lasted 90 seconds. The transducers' output signals were collected and processed by the data acquisition system already used for the wall temperature measurements.

When the measurements were finished, average air temperature and velocity, standard deviation of the velocity measured, mean radiant temperature and operative temperature were calculated for each measurement point. The mean radiant temperatures were determined for a sitting person, at a height of 0.6 m above the floor. The angle factors were calculated using the diagrams given in [12].

comfort are in the range from -0.5 to +0.5. The metabolic rate for light office activities was estimated at 1.2 met (1 met = 58.2 W/m^2) and summer clothing insulation at 0.5 clo (1 clo = 0.155 m^{2}K/W).

$$\begin{aligned}\mathrm{PMV} = &\left(0.303\,\mathrm{e}^{-0.036\,\mathrm{M}} + 0.028\right)\cdot\left\{\left(M-W\right) - \right.\\ &-3.05\cdot10^{-3}\left[5733-6.99\left(M-W\right)-p_{\mathrm{air}}\right]-\\ &-0.42\left[\left(M-W\right)-5815\right]-1.7\cdot10^{-5}\,M\left(5867-p_{\mathrm{air}}\right)-\\ &-0.0014\,M\left(34-\vartheta_{\mathrm{air}}\right)-3.96\cdot10^{-8}\,f_{\mathrm{cl}}\cdot\\ &\left.\cdot\left[\left(\vartheta_{\mathrm{cl}}+273\right)^4-\left(\overline{\vartheta}_{\mathrm{r}}+273\right)^4\right]-f_{\mathrm{cl}}\cdot\alpha_{\mathrm{c}}\cdot\left(\vartheta_{\mathrm{cl}}-\vartheta_{\mathrm{air}}\right)\right\}.\end{aligned} \tag{4}$$

Predicted Percentage of Dissatisfied (PPD) index establishes a quantitative prediction of the percentage of thermally dissatisfied people determined from PMV:

$$\mathrm{PPD} = 100 - 95\,e^{-\left(0.03353\,\mathrm{PMV}^4+0.2179\,\mathrm{PMV}^2\right)}. \tag{5}$$

According to Fanger, optimal value of the PPD index is 5 %, which is the minimum of the stated function.

The risk of draught can be quantified using the PD (Percentage of Dissatisfied) index [13]:

$$\mathrm{PD} = \left(34-\vartheta_{\mathrm{air}}\right)\left(w_{\mathrm{air}}-0.05\right)^{0.62}\left(0.37\,w_{\mathrm{air}}\,T_{\mathrm{I}}+3.14\right). \tag{6}$$

Turbulence intensity in % can be calculated by Eq. (7):

$$T_{\mathrm{I}} = 100\,w_{\mathrm{sd}}/w_{\mathrm{air}}\,, \tag{7}$$

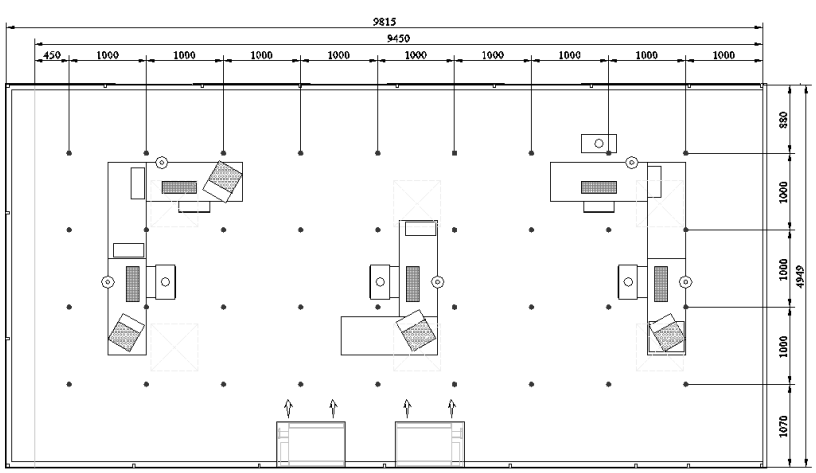

Figure 7. Measurement points in the occupied zone (•)

Slika 7. Mjerne točke u zoni boravka

Predicted Mean Vote (PMV) index [13] predicts the mean value of the votes of a large group of persons on the ASHRAE 7-point thermal sensation scale. The scale has been defined to have values from -3 (cold sensations) to +3 (warm sensations), with 0 representing neutral thermal sensation. The PMV model, given by Eq. (4), uses heat balance principles to relate the six key factors for thermal comfort (environmental parameters, metabolic rate and clothing insulation) to the average response of people on the scale. Acceptable values of the index for thermal

where w_{sd} is the standard deviation of the air velocity measured (w_{air}). The PD index is valid for air temperatures ranging from 20 to 26 °C, velocities in the range of 0.05 to 0.4 m/s and turbulent intensities lower than 70 %. For a comfortable environment, the PD index should be less than 15 %.

Effective draft temperature, ϑ_{EDT}, is the difference in temperature between any point in the occupied zone and the control condition (average temperature) [14]:

$$\vartheta_{EDT} = (\vartheta_{air} - \vartheta_c) - 8(w_{air} - 0.15), \quad (8)$$

where ϑ_{air} is air temperature and w_{air} air velocity in a measurement point, while ϑ_c is the control condition. A high percentage of people are comfortable in office occupations where the effective draft temperature as defined in Eq. (8) is between −1.7 and +1.0 °C and the air velocity is less than 0.35 m/s [14].

Air diffusion performance index, ADPI, is defined as the percentage of uniformly distributed measurement points within the occupied zone that meet those specifications for effective draft temperature and air velocity. According to ASHRAE standard, ADPI index should not be less than 80 %.

4. Results

4.1. Initial flow conditions

The jet flow characteristics were investigated under the experimental conditions listed in Table 1.

Average initial jet velocities w_0 were determined by measuring velocity profiles along the effective area near the nozzles of the COADIS units (Figure 8). Distribution of air velocities along a half of the effective area was found in nine sections with an increment of 50 mm along the Y′ axis and in 22 steps with an increment of 5 mm in the Z′ direction. Figure 9 shows the resulting velocity profiles at the middle fan speed in a non-dimensional form. The graph indicates that the velocity profiles along the effective area are not uniform. The velocity is maximal near the ceiling (usually 5 or 10 mm below it) and it gradually decreases with the distance from the ceiling to the values typically lower than 0.15 m/s.

The average turbulence intensity at the first fan speed was 10%, at the second speed 12 % and at the third one 13%. The maximum value of turbulence intensities along the effective area exceeded 25 %.

Table 1. Experimental conditions for the terminal units

Tablica 1. Pregled uvjeta pri ispitivanju terminalnih uređaja

Fan speed / Brzina vent.	$\dot{V}_{air}$, m³/h	w_0, m/s	ϑ_o, °C	ϑ_0, °C	$\Delta\vartheta$, °C	Ar	Re
1.	564	5.9	24.5	15.9	8.0	0.0021	113000
2.	393	4.4	24.6	14.5	9.6	0.0047	83300
3.	265	2.8	24.9	13.0	11.4	0.0140	52500

Average size of the effective area and supply air flow rates at each fan speed were calculated by integrating velocity profiles measured along the effective area [15]. The average length of the effective area was found to be equal to 0.807 m (R^2 = 0.010 m) and its height to 0.099 m (R^2 = 0.002 m), giving a surface of 0.080 m^2.

The calculated supply air flow rates given in Table 1 differ on average 6 % from the flow rates determined by CIAT's official measurements carried out in the accordance with the ISO 5801:1997 standard.

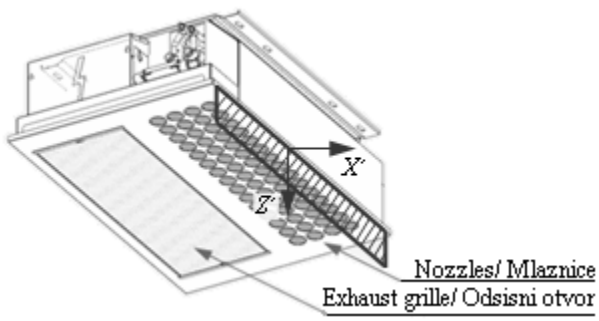

Figure 8. Effective area of the flow

Slika 8. Efektivna površina strujanja

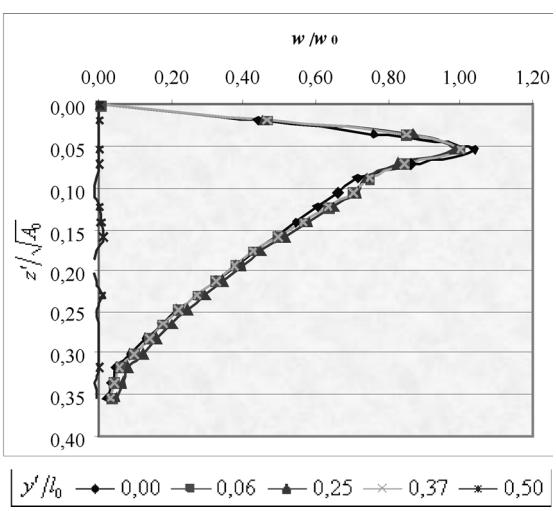

Figure 9. Non-dimensional velocity profiles along the effective area at the middle fan speed

Slika 9. Bezdimenzijski profili brzina duž efektivne površine za srednju brzinu vrtnje ventilatora

Since the ratio of the length l_0 to the height h_0 of the effective area was equal to 8.2 (i.e. $1 < l_0/h_0 < 40$), the jets produced by the COADIS units were considered to be three-dimensional. The characteristics of three-dimensional wall jets are commonly described using the parameter $\sqrt{A_0}$ [16]. The values of Archimedes and Reynolds numbers given in Table 1 were, thus, calculated according to Eq. (9) and (10) respectively:

$$\mathrm{Ar} = g\,\beta\,\Delta\vartheta\sqrt{A_0}\,/\,w_0^2, \quad (9)$$

$$\mathrm{Re} = w_0\sqrt{A_0}\,/\,\nu. \quad (10)$$

4.2. Jet characteristics downstream from the units

Figure 10 shows non-dimensional velocity profiles in different cross sections of the jet discharged at the first (highest) fan speed from the left terminal unit. Similar results were obtained for the second unit and at all fan speeds. In accordance with the air jet theory, the velocity profiles in different cross sections of the flow are similar. The shape of the profiles is very well described by the empirical equations given by Rajaratnam [16], Eq. (11), and Awbi [10], Eq. (12), for two-dimensional wall jets:

$$w_x/w_m = 1.48\left(z/z_{0.5}\right)^{1/7}\left[1-\mathrm{erf}\left(0.68\,z/z_{0.5}\right)\right], \qquad (11)$$

where $z_{0.5} = 0.068\ (x + 10h_0)$,

$$w_x/w_m = \mathrm{e}^{\left[-0.937\left(z/z_{0.5}-0.4\right)^2\right]}. \qquad (12)$$

Some discrepancies between the measured velocities and the velocities predicted by Eq. (11) and (12) were detected in the lower part of the profiles measured at further distances from the terminal unit. The discrepancies can be attributed to the (limited) dimensions of the test room used in the research. A similar shape of the lower part of the velocity profiles was reported by Karimipanah [17].

A non-dimensional form of the development of turbulence intensities in the jet discharged from the left terminal unit at the first fan speed is shown in Figure 11. An increase of turbulence intensities in the jet at further distances from the unit has a saddle shape that is characteristic for three-dimensional jets [15]. Two regions of the flow can be distinguished: one for $x'/\sqrt{A_0}$ < 3.2 and the other one for further distances from the unit. The first region is a region of characteristic velocity decay in which turbulence intensities are low. The second region is characterised by axisymmetric velocity decay. At further distances from the unit, mixing of the primary and room air is very pronounced, which is followed by intense turbulences (30 to 50 % depending on the initial jet velocity). Turbulence intensities are highest within the zone of complete decay of the jet.

The growth of the length scale ($z_{0.5}$) with the axial distance of the jet discharged at the first fan speed is shown in Figure 12 for all three analysed distances between the terminal units. In the characteristic decay region, the growth of the length scale is almost identical for all the fan speeds and distances between the units. In the axisymmetric decay region, the growth is dependent on the initial jet velocity: the growth rate is slow at the first (highest) fan speed and fast at the third speed. The slower the fan speed (i.e. initial velocity), the earlier the jet separates from the ceiling and drops towards the occupied zone, which results in growth of the length scale of the jet.

Table 2. The growth rates of the length scale of the jets

Tablica 2. Brzina porasta širine mlazova

Fan speed / Brzina vent.	Equation / Izraz	R^2
1.	$z'_{0.5}/\sqrt{A_0} = 0.184\,x'/\sqrt{A_0}$	0.903
2.	$z'_{0.5}/\sqrt{A_0} = 0.247\,x'/\sqrt{A_0}$	0.935
3.	$z'_{0.5}/\sqrt{A_0} = 0.333\,x'/\sqrt{A_0}$	0.927

Analysis of the dependence of the growth of the length scale on the distance between the terminal units

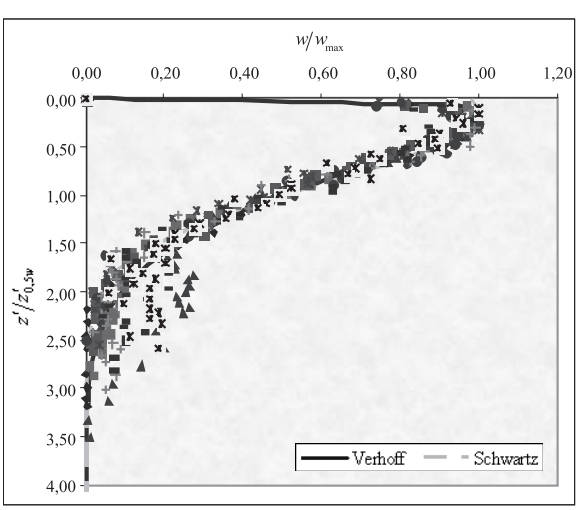

Figure 10. Typical similarity of non-dimensional velocity profiles in different cross sections of the jet

Slika 10. Tipična sličnost bezdimenzijskih profila brzina u različitim presjecima mlaza

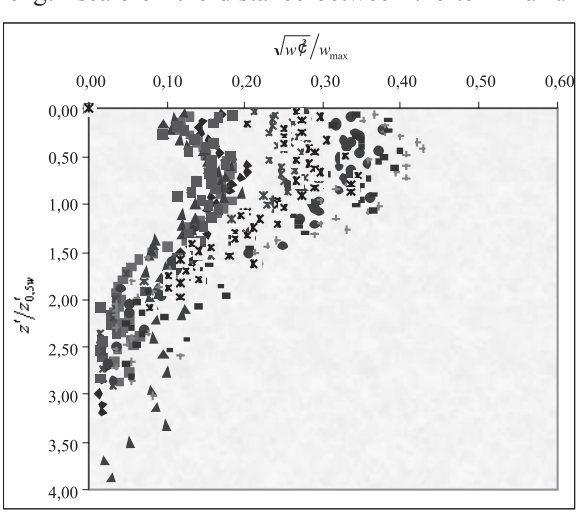

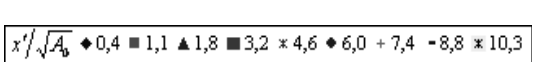

Figure 11. Typical development of turbulence intensity in the jet

Slika 11. Tipičan razvoj intenziteta turbulencija u mlazu

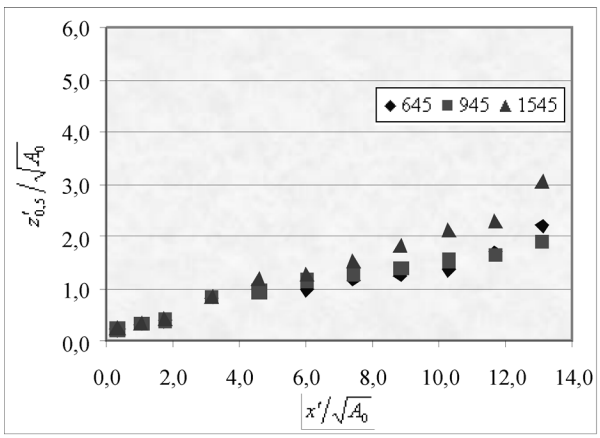

Figure 12. Growth of the length scale of the jets

Slika 12. Porast širine mlazova

at a constant initial velocity showed a weak tendency of an increase of the growth with an increase in the distance between the units. Neglecting these differences in the growth rates of the jets at different distances between the units, a regression analysis was used to model the relationship between the growth of the length scale of the jets discharged at a single fan speed and the axial distance from the units. The resulting growth rates are listed in Table 2.

Maximum velocity decay

Maximum velocity decay for three-dimensional wall jets is defined by the following general equation:

$$w_m/w_0 = K\left[\sqrt{A_0}/(x'+x_0)\right]^n. \quad (13)$$

Awbi [10] states that the exponent n in the characteristic decay region for three-dimensional wall jets discharged from the ATD with an aspect ratio of 10 is equal to 0.16. In the axisymmetric decay region, the exponent is equal to 1.15 regardless of the aspect ratio of the ATD. The aim of the following analysis was to determine the coefficients of the maximum velocity decay K and exponents n for all the fan speeds and distances between the terminal units. Since analysis of the jets structure indicated two dominated flow regions, it was necessary to find the values of these parameters separately for both of them. The analysis of the development of the centreline velocity is described in the following section, for the jet discharged from the left terminal unit at the first fan speed, while the distance between the units was 645 mm. A logarithm transformation of Eq. (13) gives:

$$\ln(w_m/w_0) = n\ln\left[\sqrt{A_0}/(x'+x_0)\right] + \ln K, \quad (14)$$

which can be presented in a linear form $y = ax + b$ and drawn in a graph such as the one shown in Figure 13. The coefficient a is equal to the exponent n, and the coefficient K is equal to e^b. Using the graph in Figure 13, linear regression functions for two clearly distinguished regions were found.

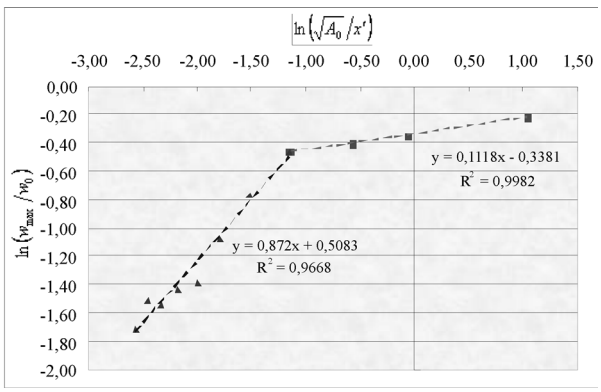

Figure 13. Development of the centreline velocity in the jet discharged from the left unit at the first fan speed

Slika 13. Razvoj maksimalne brzine u mlazu koji istrujava iz lijevoga uređaja u I. brzini vrtnje ventilatora

The centreline (maximum) velocity decay in the characteristic decay region (points marked with squares in Figure 13) is given by Eq. (15), while the decay in the axisymmetric region (points marked with triangles) is given by Eq. (16):

$$\ln(w_m/w_0) = 0.11\ln\left(\sqrt{A_0}/x'\right) - 0.34, \quad (15)$$

$$\ln(w_m/w_0) = 0.87\ln\left(\sqrt{A_0}/x'\right) + 0.51. \quad (16)$$

A parameter describing the position of the jet's virtual origin, x_0, was excluded from Eqs. (15) and (16). By equalising the left side of Eq. (15) with 0 one can obtain that $x' = x_0 = 13.7$ mm, a value that can be neglected. Since in all other analysed cases that parameter was similarly small, it was assumed that the virtual origin was exactly on the effective area. In reality, the virtual origin is near the external edge of the first row of nozzles. By arrangement of Eq. (15) and (16), the following expressions were obtained:

$$w_m/w_0 = 0.7\left(\sqrt{A_0}/x'\right)^{0.1}, \quad (17)$$

$$w_m/w_0 = 1.7\left(\sqrt{A_0}/x'\right)^{0.9}. \quad (18)$$

The velocity decay coefficient K in the characteristic decay region, for the jet discharged at the first fan speed from the left terminal unit while the distance between the units was 645 mm, was found to be 0.7 and the exponent n 0.1. In the axisymmetric decay region, the coefficient K was found to be 1.7 and the exponent n 0.9. The described procedure was used for determining centreline velocity decay parameters for all the other analysed configurations.The resulting velocity decay coefficients K and exponents n in the characteristic region were found

to be almost equal in all the tests. In this region all the jets behave in a similar manner, independently on the initial velocity and the distance between the units. Average value of the exponent *n*, taking into account all the results, was 0.1, which is a somewhat smaller value than the value found in the literature (0.16). The smaller value means that the centreline velocity decay in the analysed jets was slower and the throw longer. The difference in the values could be a consequence of different aspect ratios of the openings used (8.2 compared to 10); a consequence of the interaction of the jets produced by the terminal units used in the present research, which generally results in increased throw; and a consequence of the dimensions of the test room.

In the axisymmetric decay region, maximum velocity decay is dependent on the initial velocity. The slower the fan speed, the more pronounced the centreline velocity decay is. The exponents *n* had values between 0.6 and 1.2. These values are also somewhat smaller than the value found in the literature (1.15).

Regardless of the differences in the structure of the analysed jets, for purely practical reasons, the development of the centreline velocity was described by one common equation for the characteristic decay region and a similar equation for the region of axisymmetric velocity decay. The average velocity decay coefficient in the characteristic region was found to be 0.7 and the exponent *n* 0.1. In the axisymmetric region, the average velocity decay coefficient was equal to 1.6 and the exponent *n* to 0.9. The following equations apply (see also Figure 14):

$$w_m / w_0 = 0.7\left(\sqrt{A_0}/x'\right)^{0.1},\ R_2 = 0.79; \tag{19}$$

$$w_m / w_0 = 1.6\left(\sqrt{A_0}/x'\right)^{0.9},\ R_2 = 0.88. \tag{20}$$

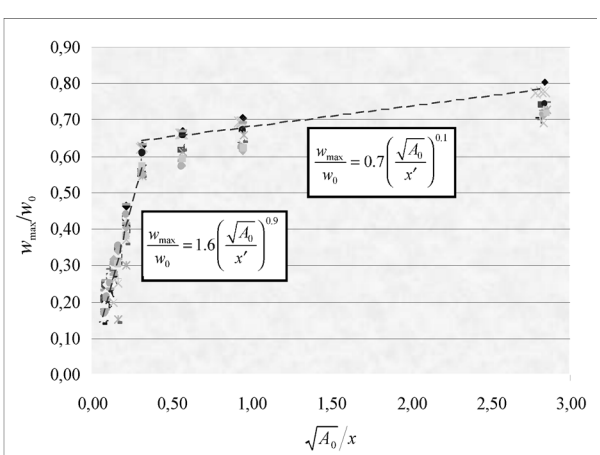

Figure 14. Development of the centreline velocity in all the analysed jets

Slika 14. Razvoj maksimalne brzine u svim analiziranim mlazovima

Distance of separation from the ceiling

Separation distance for a wall jet is difficult to predict precisely, because it is dependent on the space geometry and the internal loads. Various experimental studies have shown that the separation distance x'_{sep} can be expressed as a function of Archimedes number [15]. Comparing the results obtained in the present research with Rutman's results [15], a similarity was noticed. Taking both sets of the results into account, the following regression equation was obtained ($R^2 = 0.96$):

$$x'_{sep} / \sqrt{A_0} = 0.45\,\mathrm{Ar}^{-0.6}. \tag{21}$$

4.3. Evaluation of thermal comfort

Average values of the relevant parameters used for the evaluation of thermal comfort are given in Table 3. The percentages of measurement points that satisfied the specifications prescribed by the international standards [18] for each parameter are given in Table 4. The results refer to the second (2.) and third (3.) fan speed.

The average air temperature in the occupied zone, was lower than planned 25 °C in all the tests. This suggests that the balance between the cooling capacity of the terminal units and heat loads in the test room was not sufficiently achieved. The cooling capacity provided by the COADIS units was slightly higher than required. Regardless of that fact, the average operative temperature was always around 24.5 °C.

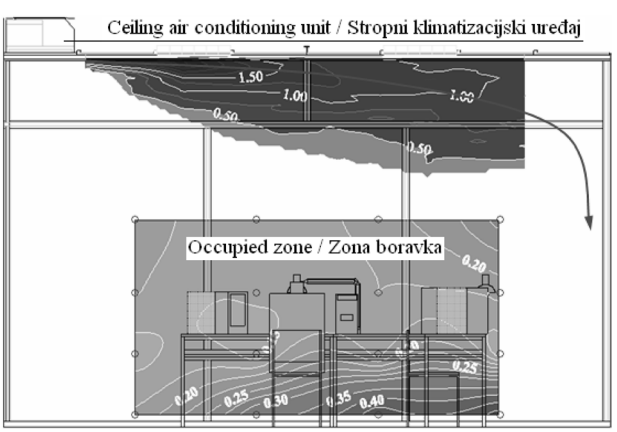

Figure 15. Air velocities in the jet and in the occupied zone at the middle fan speed

Slika 15. Brzine strujanja zraka u mlazovima i u zoni boravka pri srednjoj brzini vrtnje ventilatora

Figure 15 shows the results of velocity measurements in the cross section of the test room passing through the centre of the left terminal unit. The results refer to the measurements performed at the second fan speed and the distance between the units 645 mm. The results were graphically represented using the Golden Software's

Surfer 7.02. Velocity profiles in the jets in the vicinity of the external wall of the test room (the right wall in Figure 15) could not be measured, since the LDA probe could not be placed there due to the dimensions of the traversing system. The results show that the air discharged from the unit remained attached to the ceiling until the external wall was reached, which finally turned the air down towards the floor. The analysis of the air velocity distribution at the first and second fan speeds showed that the jets adhered to the external wall and continued to flow within the occupied zone. At the first fan speed, the velocities at a height of 100 mm above the floor ranged from 0.6 m/s near the external wall to about 0.25 m/s near the opposite end of the occupied zone. At the second fan speed the velocities were only slightly lower. Besides that, due to insufficient mixing of the primary and room air, the air temperatures near the floor were unacceptably low. High air velocities and low temperatures inevitably lead to the feeling of draught and the application of these two fan speeds should be avoided when designing an air conditioning system for a room of similar project conditions like in the research. The most acceptable microclimate conditions in the occupied zone were obtained when the terminal units operated at the lowest, third fan speed. In this case, the jet separated from the ceiling before reaching the external wall and dropped towards the floor. Good mixing with the room air provided lower air velocities and higher temperatures, guaranteeing a high level of thermal comfort.

Table 3. Measured values of thermal comfort parameters

Tablica 3. Izmjerene vrijednosti parametara ugodnosti

Parameter / Parametar	Distance between units / Udaljenost između jedinica, mm		
	645	945	1545
	2./3.	2./3.	2./3.
$\overline{\vartheta}_{air}$, °C	24.1/24.4	24.0/24.3	24.1/24.5
$\overline{\vartheta}_{r}$, °C	25.1/25.5	25.1/25.3	25.2/25.5
ϑ_{o} , °C	24.6/24.9	24.5/24.8	24.6/25.0
$\overline{w}_{air}$, m/s	0.189/0.138	0.188/0.139	0.181/0.147
PMV	-0.3/-0.1	-0.3/-0.1	-0.2/0
PPD, %	8.3/6.2	8.5/6.4	7.8/6.2
PD, %	17.7/11.3	17.4/11.7	16.8/12.4
ϑ_{EDT} , °C	-0,31/0.10	-0,30/0.09	-0,25/0.02
ADPI, %	77.1/81.9	76.4/77.1	78.5/85.4

Table 4. Percentage of locations that satisfy the prescribed condition of a thermal comfort parameter

Tablica 4. Postoci mjernih točaka u kojima je zadovoljen uvjet parametra ugodnosti

Parameter / Parametar	Distance between units / Udaljenost između jedinica, mm		
	645	945	1545
	2./3.	2./3.	2./3.
ϑ_{o} , (24.5±1.5, °C)	99/99	99/98	100/99
w_{air} (<0.22 m/s)	74/84	74/83	74/82
PD (<20 %)	72/84	73/83	74/82
PMV (-0.5÷0.5)	78/94	78/92	80/94
PPD (<10 %)	78/94	76/92	79/93

5. Conclusion

To optimize performances of a building HVAC system in the design phase, reliable numerical models must be used. These models must be fast and easily handled by system designers, yet giving them the most relevant information on the systems performances. To accelerate and simplify their usage, complex mathematical models consisting of partial differential equations for heat transfer and fluid flow are commonly substituted with empirical correlations and coefficients. These must be obtained by carrying out experimental measurements or, under certain conditions, validated CFD simulations.

The aim of the presented research was to describe and quantify the main characteristics of the wall jets discharged from commercially available terminal devices. Velocity profiles in the jets, maximum velocity decays, turbulence intensities and growth rates were analysed and mathematically described. These equations can be implemented in numerical models and bring the necessary simplification on one side, and reliability on the other. In the second phase of the research, measurements in the occupied zone were performed to map air velocity and temperature fields. The first goal of this phase was to check the influence of the wall jets on thermal comfort in the office, while the second goal was to build a database of measurement results that could be used for validation of different types of numerical models developed.

The experimental results implied that the distance between the terminal units had no significant impact on the overall thermal comfort. This issue has to be investigated further.

Acknowledgments

This paper is result of an investigation made in the frame of scientific research project “Research and

Development of Components and Systems of Renewable Energy Sources", supported by Ministry of Science, Education and Sports. / Rad je rezultat istraživanja u okviru znanstveno-istraživačkog projekta "Istraživanje i razvoj komponenata i sustava obnovljivih izvora energije", koji financira Ministarstvo znanosti, obrazovanja i športa.

REFERENCES

[1] CHARLES, K. E.: *Office Air Distribution Systems and Environmental Satisfaction*, IRC-RR-161, Institute for Research in Construction, National Research Council Canada, 2002.

[2] WYON, D. P.: *The Effects of Indoor Air Quality on Performance and Productivity*, Indoor Air 2004; 14 (Suppl. 7), Blackwell Munksgaard 2004, 92-101.

[3] TOFTUM, J.; ANDERSEN, R. V.; JENSEN, K. L.: *Occupant Performance and Building Energy Consumption with Different Philosophies of Determining Acceptable Thermal Conditions*, Building and Environment, doi:10.1016/j.buildenv.2009.02.007

[4] ...: *Energetska učinkovitost u zgradarstvu*, HEP Toplinarstvo d.o.o. i Energetski institut Hrvoje Požar, Zagreb, 2007.

[5] YANG, B.: *Thermal Comfort and Indoor Air Quality Evaluation of a Ceiling Mounted Personalized Ventilation System Integrated with an Ambient Mixing Ventilation System*, PhD thesis, National University of Singapore, 2009.

[6] INARD, C.; BOUIA, H.; DALICIEUX, P.: *Prediction of Air Temperature Distribution in Buildings with a Zonal Model*, Energy and Buildings 24, 1996., 125-132.

[7] DAOUD, A.; GALANIS, N.: *Prediction of Airflow Patterns in a Ventilated Enclosure with zonal methods*, Applied Energy 85, 2008., 439-448.

[8] VILIČIĆ, I.: *Distribucija zraka kroz rešetke direktno priključene na kanal*, Strojarstvo: časopis za teoriju i praksu u strojarstvu, Vol. 20, 1978., 355-363.

[9] RECKNAGEL, H.; SPRENGER, E.; SCHRAMEK, E.-R.: *Taschenbuch für Heizung + Klimatechnik* 05/06, R. Oldenbourg Industrieverlag GmbH, München, 2004.

[10] AWBI, H. B.: *Ventilation of Buildings*, Spon Press, Taylor and Francis Group, London, 2003.

[11] ...: *Laser Doppler Anemometry - Introduction to Principles and Applications*, Dantec Dynamics A/S, 2002.

[12] ASHRAE: *Chapter 8: Thermal Comfort*, ASHRAE Fundamentals Handbook (SI), 2005.

[13] FANGER, P. O.: T*hermal Comfort Analysis and Applications in Environmental Engineering*, McGraw-Hill Book Company, New York, 1972.

[14] ASHRAE: *Chapter 32: Space Air Diffusion*, ASHRAE Fundamentals Handbook (SI), 2002.

[15] RUTMAN, E.: *Contribution à l' évaluation de la qualité des ambiances intérieures climatisées*, PhD thesis, Université de la Rochelle, 2000.

[16] RAJARATNAM, N.: *Turbulent Jets*, Elsevier Scientific Publishing Company, Amsterdam, 1976.

[17] KARIMIPANAH, T.: *Turbulent Jets in Confined Spaces*, PhD thesis, Royal Institute of Technology, KTH, 1996.

[18] WOLF, I.: *Modeli predviđanja toplinske ugodnosti prostora*, Strojarstvo: časopis za teoriju i praksu u strojarstvu, Vol. 51 (5), 2009., 507-517.